

Supplementary Information: 3D-UnOutDet: A Fast and Efficient Unsupervised Snow Removal Algorithm for 3D LiDAR Point Clouds

Abu Mohammed Raisuddin¹, Idriss Gouigah¹ and Eren Erdal Aksoy¹

S1. WINTER ADVERSE DRIVING DATASET

Regarding Winter Adverse Driving Dataset, please refer to the Supplementary information of 3D-OutDet [1] at https://github.com/sporsho/sporsho.github.io/blob/main/Suppli_3D_OutDet.pdf

S2. RUNTIME OF LISNOWNET

Regarding the runtime of LiSnowNet [2], please refer to the Supplementary information of 3D-OutDet [1] at https://github.com/sporsho/sporsho.github.io/blob/main/Suppli_3D_OutDet.pdf

S3. INPUT TYPES FOR DEEP MODELS

TABLE S1: Input Types for models

Model	Data Input
SOR [3]	Raw Point Cloud
ROR [3]	Raw Point Cloud
DSOR [4]	Raw Point Cloud
DROR [5]	Raw Point Cloud
SSR (Ours)	Raw Point Cloud
LIOR [6]	Raw Point Cloud
LiSnowNet [2]	Range View
SalsaNext [7]	Range View
SLiDE [8]	Range View
SSEDEn / SMEDEn [9]	Range View
PolarNet [10]	Polar Birds Eye View
Cylinder3D [11]	Cylindrical 3D voxel

S4. THRESHOLDING VALUE FOR SSR

Though WADS do provide point-wise annotation, we cannot use them to find the optimal thresholding value as our algorithm is unsupervised. Hence we empirically decided the threshold value. For that we visualized the SSR results for five different thresholds (0, 2.5, 5.0, 7.5 and 10.0). In Figure S1a we see that no snow is detected at threshold 0. In Figure S1b, we see that a good amount of snow is detected along with some false predictions. We highlighted the false positives as the green points inside red ellipses and false negatives as the black points inside blue rectangles. Black

*This work was funded by the European Union (grant no. 101069576). Views and opinions expressed are however those of the author(s) only and do not necessarily reflect those of the European Union or the European Climate, Infrastructure and Environment Executive Agency (CINEA). Neither the European Union nor the granting authority can be held responsible for them.

¹Halmstad University, School of Information Technology, Center for Applied Intelligent Systems Research, Halmstad, Sweden
abu-mohammed.raisuddin@hh.se

points are predicted snow and green points are predicted non-snow points. Figure S1c, S1d, S1e shows the visualization for thresholds 5.0, 7.5, and 10.0 respectively. From the figures we noticed that as we increase the threshold value above 2.5, the number of False negatives and False positives also increases. Hence, we have chosen 2.5 as the threshold value for WADS dataset.

S5. ABOUT INVERSE SQUARE LAW OF LIGHT INTENSITY

Equation 1 shows the equation of Inverse Square Law of Light Intensity. So, multiplying intensity with distance squared will result in a constant. Though, LiDAR captures the returned intensity, not the intensity at the object, multiplying the intensity with distance will stabilize the value from fluctuation giving an easier thresholding opportunity.

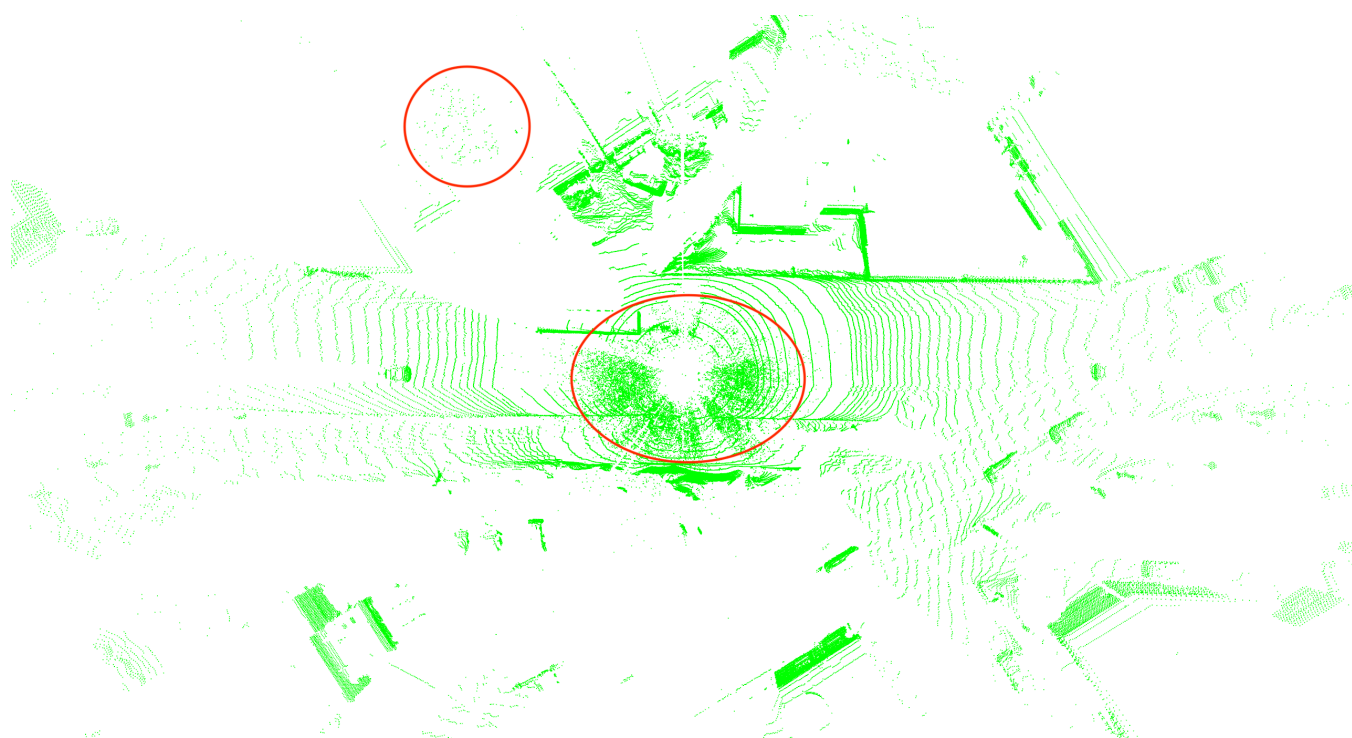
$$Intensity \propto \frac{1}{distance^2} \quad (1)$$

S6. LABELING CADC

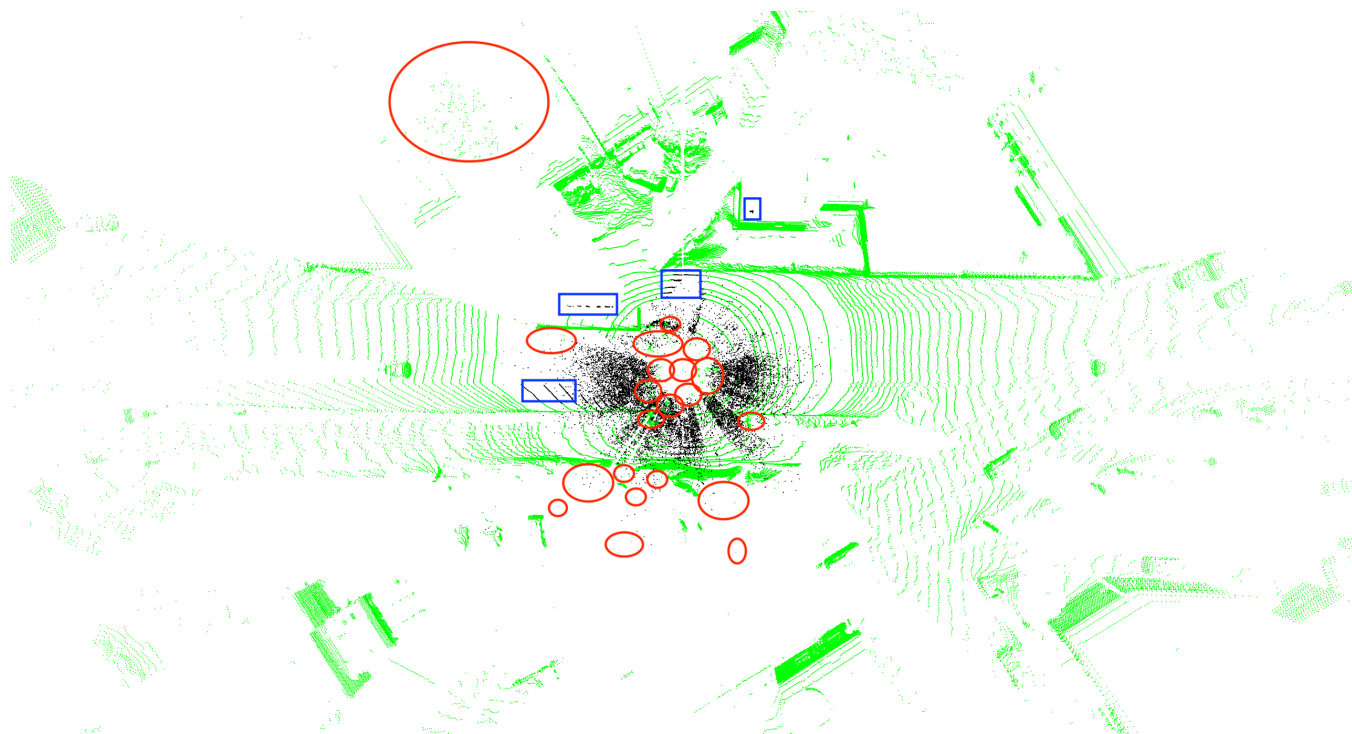
2 sequences of CADC dataset were labeled by human and with this two sequences we trained 2-fold cross validation models. E.g., for model1, we used first sequence for training and the second one for validation and for model2, we used the second sequence for training and the first sequence for validation. Then we used the average of prediction probability from this two models to generate the labels of the test set. We note that there are 32 sequences in the test set and 2 of them are annotated, hence remaining 30 sequences are machine annotated. To see how agreeable the machine annotations are in comparison with human annotation, we conducted Cohen's Kappa [12] analysis and for the two sequences that are annotated by both human and machine have a quadratic kappa score of 0.9796. Kappa score ranges from -1 to 1 where 1 means complete agreement and values near zero means that the agreement is by chance, -1 indicates complete disagreement. We see that our machine generated labels are quite agreeable with human annotations.

REFERENCES

- [1] A. M. Raisuddin, T. Cortinhal, J. Holmblad, and E. E. Aksoy, "3d-outdet: A fast and memory efficient outlier detector for 3d lidar point clouds in adverse weather," in *2024 IEEE Intelligent Vehicles Symposium (IV)*. IEEE, 2024, pp. 2862–2868.
- [2] M.-Y. Yu, R. Vasudevan, and M. Johnson-Roberson, "Lisnownet: Real-time snow removal for lidar point clouds," in *2022 IEEE/RSJ International Conference on Intelligent Robots and Systems (IROS)*. IEEE, 2022, pp. 6820–6826.
- [3] R. B. Rusu and S. Cousins, "3d is here: Point cloud library (pcl)," in *2011 IEEE international conference on robotics and automation*. IEEE, 2011, pp. 1–4.

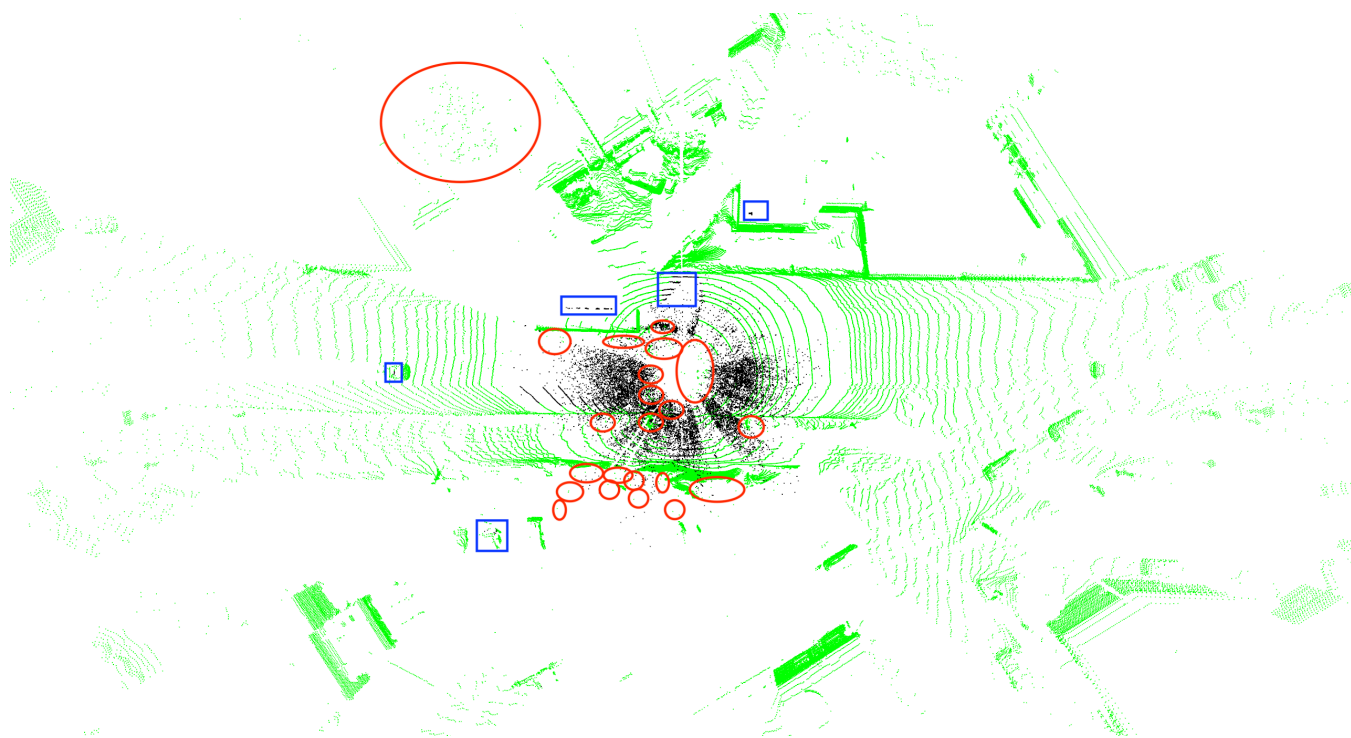


(a) SSR Thresholding at 0.0

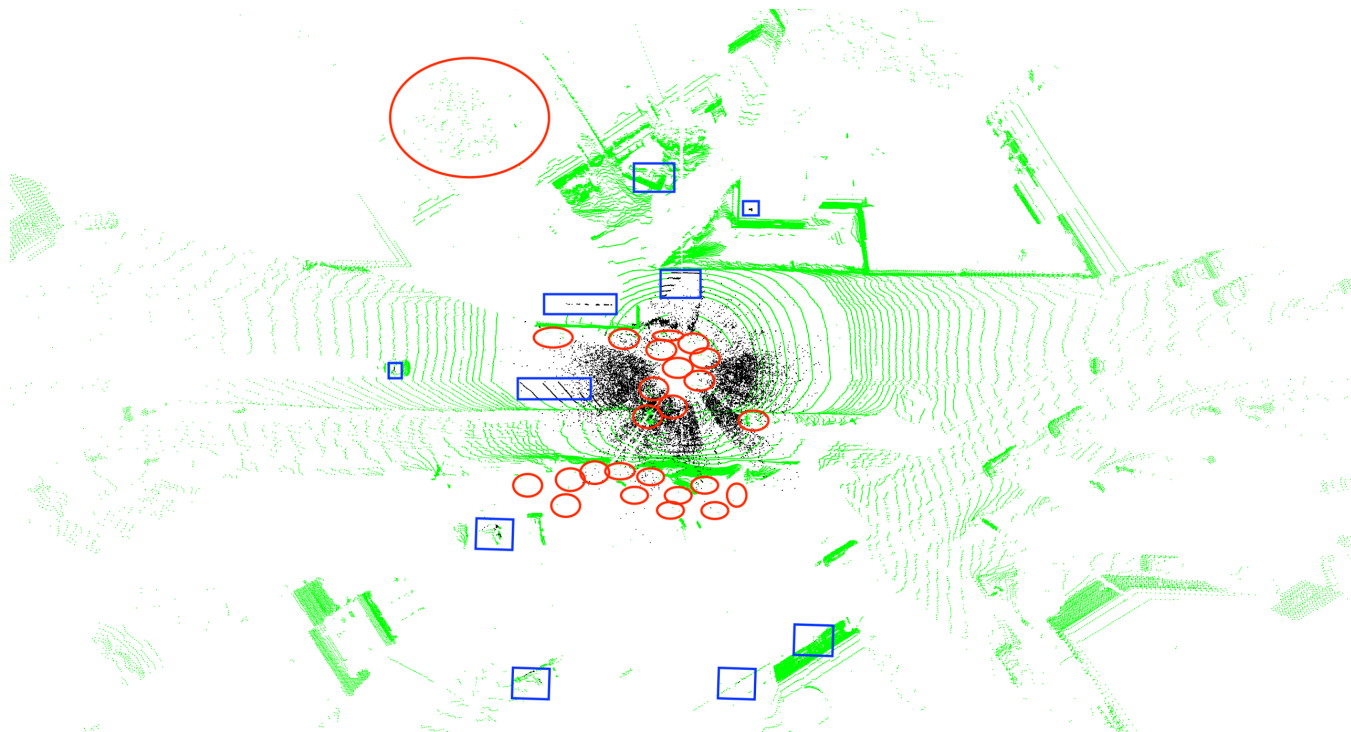


(b) SSR Thresholding at 2.5

Fig. S1: SSR on WADS. Green points inside red ellipses are false positives, black dots inside blue rectangle are false negatives



(c) SSR Thresholding at 5.0



(d) SSR Thresholding at 7.5

Fig. S1: SSR on WADS. Green points inside red ellipses are false positives, black dots inside blue rectangle are false negatives

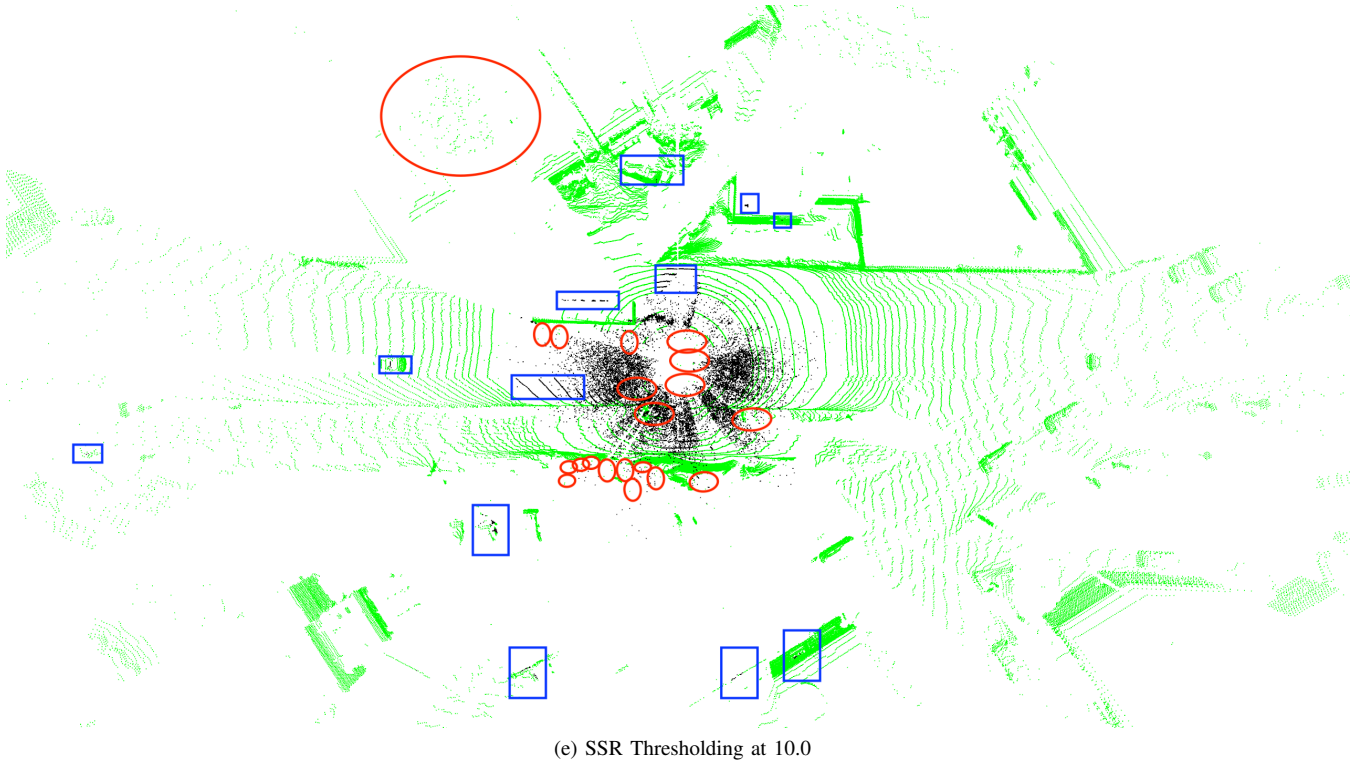


Fig. S1: SSR on WADS. Green points inside red ellipses are false positives, black dots inside blue rectangle are false negatives

- [4] A. Kurup and J. Bos, "Dsor: A scalable statistical filter for removing falling snow from lidar point clouds in severe winter weather," *arXiv preprint arXiv:2109.07078*, 2021.
- [5] N. Charron, S. Phillips, and S. L. Waslander, "De-noising of lidar point clouds corrupted by snowfall," in *2018 15th Conference on Computer and Robot Vision (CRV)*. IEEE, 2018, pp. 254–261.
- [6] J. il Park, J. Park, and K.-S. Kim, "Fast and accurate desnowing algorithm for lidar point clouds," *IEEE Access*, vol. 8, pp. 160 202–160 212, 2020.
- [7] T. Cortinhal, G. Tzelepis, and E. Erdal Aksoy, "Salsanext: Fast, uncertainty-aware semantic segmentation of lidar point clouds," in *International Symposium on Visual Computing*. Springer, 2020, pp. 207–222.
- [8] G. Bae, B. Kim, S. Ahn, J. Min, and I. Shim, "Slide: Self-supervised lidar de-snowing through reconstruction difficulty," in *European Conference on Computer Vision*. Springer, 2022, pp. 283–300.
- [9] A. Seppänen, R. Ojala, and K. Tammi, "Self-supervised multi-echo point cloud denoising in snowfall," *Pattern Recognition Letters*, vol. 185, pp. 52–58, 2024.
- [10] Y. Zhang, Z. Zhou, P. David, X. Yue, Z. Xi, B. Gong, and H. Foroosh, "Polarnet: An improved grid representation for online lidar point clouds semantic segmentation," in *Proceedings of the IEEE/CVF Conference on Computer Vision and Pattern Recognition*, 2020, pp. 9601–9610.
- [11] H. Zhou, X. Zhu, X. Song, Y. Ma, Z. Wang, H. Li, and D. Lin, "Cylinder3d: An effective 3d framework for driving-scene lidar semantic segmentation," *arXiv preprint arXiv:2008.01550*, 2020.
- [12] J. Cohen, "A coefficient of agreement for nominal scales," *Educational and psychological measurement*, vol. 20, no. 1, pp. 37–46, 1960.